Memorie della

Study of the M shock wave propagation in RXJ1314.4–2515

P. Mazzotta[1,2], H. Bourdin[1], S. Giacintucci[2], M. Markevitch[2], and T. Venturi[3]

[1] Dipartimento di Fisica Università di Roma "Tor Vergata", Via della ricerca scientifica 1, I-00133 Roma, Italy, e-mail: `mazzotta@roma2.infn.it`
[2] Harvard-Smithsonian Center for Astrophysics, 60 Garden St., Cambridge, MA 02138
[3] INAF – Istituto di Radioastronomia, Via Gobetti 101, I–40129, Bologna, Italy

Abstract. We present the analysis of *XMM–Newton* observations of the merging cluster of galaxies RXJ1314.4–2515. The cluster is known to host a small radio halo at its center and two Mpc-size relics in the outskirts, one to the east and one to the west. The *XMM–Newton* observation reveals the presence of a shock underlying the western relic. The outer border of the relic is remarkably coincident with the shock front. This provides important support to the shock (re)acceleration models as likely mechanisms behind the formation of the radio relics in clusters. Very interestingly the shock, which seems to propagate with a Mach number of 2.5, also shows an M–like shape with the nose of the front slightly tilted inward which is likely produced by the material infalling along the filament.

Key words. Galaxies: clusters: general – Galaxies: clusters: individual (RXJ1314.4–2515) – X-rays: galaxies

1. Introduction

Most of the enormous kinetic energy of cluster mergers is dissipated as heat via shocks. Shock fronts can be observed in the X–ray images as sharp brightness discontinuities associated with a gas temperature jump (e.g. Markevitch & Vikhlinin, 2007, and references therein). A fraction of the merger energy is expected to be dissipated also in turbulence. Shocks and turbulence may in turn amplify the cluster magnetic fields (Dolag et al., 2002) and accelerate ultrarelativistic particles (e.g. Brunetti, 2009, and references therein). Radio relics are believed to be due to Fermi acceleration of relativistic electrons at merger shocks

(Ensslin et al., 1998; Hoeft & Brüggen, 2007). Alternatively shocks may *revive* fossil radio plasma through adiabatic compression of the magnetic field or reaccelerate pre-existing relativistic electrons in the intracluster medium (Markevitch et al., 2005).

According to the above framework, radio relics can be potentially used as tracers of merger shocks and provide important information on the thermal gas properties in regions where the X–ray emission is often too faint to identify shock fronts.

The potential of relics is even more important if we consider that X–ray observable shock fronts are rare: only six examples of clear shock fronts, with both a gas density edge and an unambiguous temperature jump, have been published so far, i.e., 1E 0657-56 and A520

(e.g. Markevitch & Vikhlinin, 2007), and, more recently, the two shocks in A2146 (Russell et al., 2010), and those in A754 (Macario et al., 2011), A2744 (Owers et al., 2011) and A521 (Bourdin et al. in preparation).

In this paper we present the results of two *XMM–Newton* observations of the massive galaxy cluster RXCJ1314.4–2515 at z=0.244 which we compare to the 610 MHz observation made with the *Giant Metrewave Radio Telescope (GMRT)* (Venturi et al., 2007).

We use $H_0 = 70$ km s^{-1} kpc^{-1}, $\Omega = 0.27$, and $\Lambda = 0.73$, so at the cluster redshift of z=0.244, $1'' = 3.66$kpc.

2. Results

2.1. X-ray and radio images

In Fig. 1 we show the *XMM–Newton* photon image of RXJ1314.4–2515 in the [0.5,2.5] keV band. The photons from all the 3 cameras and for both observations are background subtracted, vignetted corrected, and smoothed with a Gaussian filter with sigma=2 pixels. RXJ1314.4–2515 is quite elongated in the East-West direction and does not show a clear X–ray peak in the surface brightness. On the west side with respect the cluster center we notice the presence of two abrupt variation of the surface brightness: one inner and one more external at $\approx$ 95arcsec and $\approx$ 135arcsec ($\approx$ 500kpc) from the cluster centroid, respectively. To highlight the second abrupt surface brightness variation in Fig 1 we overlay the isocontour that corresponds to the feature.

The cluster was also observed with the *VLA* at 1.4 GHz by Feretti et al. (2005) and with the *GMRT* at 610 MHz by Venturi et al. (2007). Both observations revealed the presence of a small radio halo and two relics. In Fig.1 we overlay the contour image of the 610 MHz observation. The two radio relics extend in the SE-NW direction for approximately $\sim$ 900 kpc.

It important to notice that the western relic is located in the region of the shock, and its outer border is remarkably coincident with the shock front.
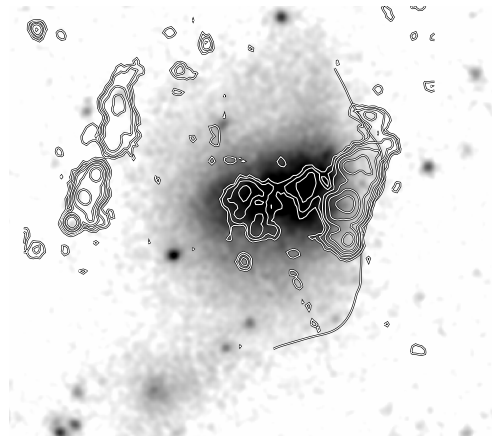

Fig. 1. *XMM–Newton* X-ray photon Gaussian smoothed image of RXJ1314.4–2515 in the [0.5,2.5] keV band. Each pixel corresponds to $1.76'' \times 1.76''$. The line is an isocontour level of the photon image that delineates the shock front. The black–white contours are the 610 MHz radio emission logarithmically spaced by a factor of 2 from $0.18 mJy\, b^{-1}$. The radio beam is $25'' \times 22''$
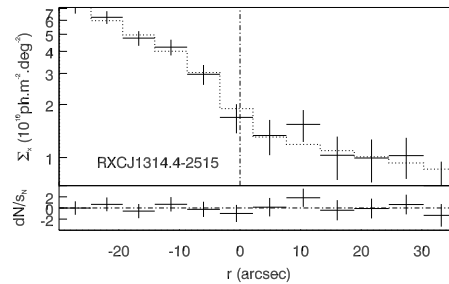.

Fig. 2. *Upper panel*) Projected surface brightness profile of the cluster sector containing the nose of the shock front in RXJ1314.4–2515. The vertical dashed–dotted line indicate the positions of the shock. The continuous histogram is the projected best fit models shown in Fig .3. *Bottom panel*) Residuals of the surface brightness profile with respect to the best fit model in sigmas.

3. Shock front

In this Section we demonstrate that the edge indicated by the line in Fig. 1 is a shock front. We extracted the surface brightness and temperature profiles within a sector centered in the

Table 1. Parameters of the Shock Front

Sector	x, y(J2000)	Pos. angle(deg)	r_{jump}(Mpc)	D_n	α_1	α_2
Center	(13 : 14 : 54.814, −25 : 14 : 06.46)	341–348	2.03 ± 0.006	2.4 ± 0.1	$6.6^{+1.3}_{-0.9}$	$2.85^{+0.9}_{-0.2}$

curvature center identified by the edge itself. The center and position angles of the sector are reported in Tab. 1.

In Fig. 2 we show the surface brightness profile of the sector. For convenience we indicate the position of the edge with a vertical dashed–dotted line. We modeled the edge using a simple analytic function for the electron density (n_e) and 3D temperature (T), both with a discontinuity (a jump) at the front:

$$n_e = n_0 \begin{cases} D_n(r/r_{jump})^{\alpha_1} & r < r_{jump} \\ (r/r_{jump})^{\alpha_2} & r > r_{jump} . \end{cases} \quad (1)$$

Assuming spherical symmetry, we projected both density and temperature models and fitted them simultaneously to the observed surface brightness and temperature profiles. We assumed a thermal emission (mekal model) for the ICM with a metallicity given by the cluster mean value. The brightness profile was obtained by convolving the projected model with the *XMM–Newton* instrumental response. Finally for the temperature projection we used the spectroscopic like definition T_{sl} introduced by Mazzotta et al. (2004).

If Fig. 3 and Fig. 4 we show the best fit within the 68% confidence level error curves relative to the density and temperature profiles, respectively. In Fig. 2 we also report as solid line the best fit models of the surface brightness, to highlight the good agreement between the fit and the data. This is also clear from the lower panel of the same figure where we show the departures in sigmas of the surface brightness data with respect to the best fit.

This analysis confirm that the observed edge is a shock front.

Using the Rankine-Hugoniot jump conditions (e.g., Landau & Liftshit's, 1959) we can derive the Mach number of the shock, $M \equiv v/c_s$, where c_s is the velocity of sound in the pre-shock gas and v is the velocity of that gas w.r.t. the shock surface, from the measured density jump at the shock:

$$M = \left[\frac{2D_n}{\gamma + 1 - D_n(\gamma - 1)} \right]^{1/2} . \quad (2)$$

If we assume that the adiabatic index is $\gamma = 5/3$ we find that the observed density jump corresponds to a Mach number $M = 2.1 \pm 0.1$ in good agreement with the estimate obtained from the radio analysis (see section 4.2).
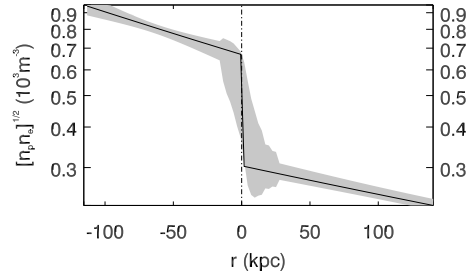

Fig. 3. Electron density (n_e) profile of the cluster sector containing the nose of the shock. The shadow region indicate the relative 68% confidence level errors.

4. Discussion

4.1. The major merger in RXJ1314.4–2515

All the data discussed in the previous sections clearly indicate that RXJ1314.4–2515 is undergoing a major merger with a subcluster traveling from East to West. The subclump has already passed the cluster center and, as for the Bullet cluster (Markevitch & Vikhlinin, 2007)

and for A2163 (Bourdin et al., 2011), it is likely that the gas of the moving subcluster has been detached from its original dark matter halo.
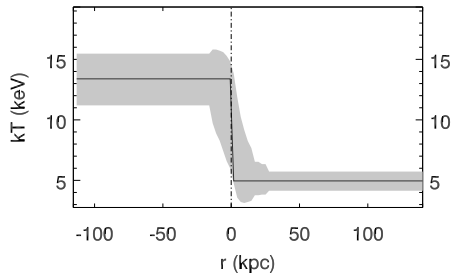

Fig. 4. Temperature (T) profile of the cluster sector containing the nose of the shock. The shadow region indicate the relative 68% confidence level errors.

4.2. Shock/relic connection

Radio relics are thought to form in proximity of shocks fronts (Ensslin et al., 1998; Roettiger et al., 1999; Hoeft & Brüggen, 2007), and therefore they are expected to trace the geometry of ongoing mergers (e.g. Clarke & Ensslin, 2006). Based on the assumption of a connection with shocks, a number of models have been proposed to explain the origin of radio relics. One possibility is the direct shock acceleration: relics are produced by electrons accelerated from the thermal gas to relativistic energies by the shock (Ensslin et al., 1998; Roettiger et al., 1999; Hoeft & Brüggen, 2007; van Weeren et al., 2010). Assuming linear shock acceleration theory, in the case of a fully ionized plasma as the ICM, the steady state energy spectrum of the electrons in the relic is a power law whose slope δ is related to the shock Mach number M according to the following equation (e.g. Blandford & Eichler, 1987):

$$\delta = 2\frac{M^2 + 1}{M^2 - 1} + 1, \tag{3}$$

where we include the the effect of particle aging ($\Delta(\delta) = 1$) from the combined effect of Inverse Compton energy losses and continuous injection (Sarazin 1999). The ensuing integrated radio emission of the relic has a single power law spectrum with $\alpha = (\delta - 1)/2$, which is thus related to the Mach number of the shock through Eq. 3. In the case of RXCJ 1314.4–2515, both relics have a total spectral index of $\alpha = 1.4$. Thus, the requested Mach number of the shock is $M \sim 2.5$.

4.3. The M–like shape of the shock front

It is interesting to notice that the shock, which seems to propagate with a Mach number of 2.5, shows an M–like shape with the nose of the front slightly tilted. This indicate that the fluid in which the shock is propagating is moving with an higher speed in the direction axes of symmetry and lower as we move away form it. Such differential velocity of the gas can be easily induced by the accretion of material falling into the clusters along the accretion filament.

References

Blandford, R., & Eichler, D., 1987, Phys. Rep., 154, 1
Bourdin, H., et al., 2011, A&A, 527, A21+
Brunetti, G., 2009, A&A, 508, 599
Clarke, T. E., & Ensslin, T. A., 2006, AJ, 131, 2900
Dolag, K., et al., 2002, A&A, 387, 383
Ensslin, T. A., et. al., 1998, A&A, 332, 395
Hoeft, M. & Brüggen, M. 2007, MNRAS, 375, 77
Landau, L. D., & Liftshit's, E. M., 1959, *Theory of Elasticity*, Addison-Wesley physics books, 89
Macario, G., et al., 2011, ApJ, 728, 82
Markevitch, M., et al., 2005, ApJ, 627, 733
Markevitch, M., & Vikhlinin, A., 2007, Phys. Rep., 443, 1
Mazzotta, P., et al., 2004, MNRAS, 354, 10
Owers, M. S., et al., 2011, ApJ, 728, 27
Roettiger, K., et al., 1999, ApJ, 518, 603
Russell, H. R., et al., 2010, MNRAS, 406, 1721
Venturi, T., et al., 2007, A&A, 463, 937
van Weeren, R. J., et al., 2010, Science, 330, 347